Respiratory Physiology & Neurobiology 263 (2019) 20–25

Contents lists available at ScienceDirect

Respiratory Physiology & Neurobiology

journal homepage: www.elsevier.com/locate/resphysiol

TRPM8 channel is involved in the ventilatory response to CO_2 mediating hypercapnic Ca^{2+} responses

Yutaka Hirata[a,*], Yoshiro Suzuki[b,c], Makoto Tominaga[b,c], Yoshitaka Oku[a,*]

[a] Department of Physiology, Hyogo College of Medicine, 1-1 Mukogawa-cho, Nishinomiya, 663-8501, Japan
[b] Division of Cell Signaling, National Institute for Physiological Sciences (Exploratory Research Center for Life and Living Systems), National Institutes of Natural Sciences, Okazaki, Aichi, 444-8787, Japan
[c] Department of Physiological Sciences, SOKENDAI (The Graduate University for Advanced Studies), Okazaki, Aichi, 444-8787, Japan

ARTICLE INFO

Keywords:
Whole-body plethysmography
Ventilatory response
Central chemosensitivity
CO_2
TRP channels

ABSTRACT

The role of TRP channels in the ventilatory response to CO_2 was investigated *in vivo*. To this end, the respiration of unrestrained adult TRPM8-, TRPV1- and TRPV4-channel knockout mice was measured using whole-body plethysmography. Under control conditions and hyperoxic hypercapnia, no difference in respiratory parameters was observed between adult wild-type mice and TRPV1- and TRPV4-channel knockout mice. However, TRPM8-channel knockout mice showed decreased tidal volume under both hypercapnia and resting conditions. In addition, the expression of TRPM8, TRPV1 and TRPV4 mRNAs was detected in EGFP-positive glial cells in the medulla of GFAP promoter-EGFP transgenic mice by real-time PCR. Furthermore, we measured intracellular Ca^{2+} responses of TRPM8-overexpressing HEK-293 cells to hypercapnic acidosis. Subpopulations of cells that exhibited hypercapnic acidosis-induced Ca^{2+} response also responded to the application of menthol. These results suggest that TRPM8 partially mediates the ventilatory response to CO_2 via changes in intracellular Ca^{2+} and is a chemosensing protein that may be involved in detecting endogenous CO_2 production.

1. Introduction

Ventilation is regulated and maintained by the levels of O_2 and CO_2 partial pressures in the body. This regulatory process is known to involve several neuronal pathways, among which the central respiratory chemoreflex refers to ventilatory responses to increases in brain P_{CO2} (Santin, 2018; Nattie and Li, 2012). The central respiratory chemoreflex seems to be operated predominantly by the activity of retrotrapezoid nucleus (RTN) neurons, because genetic deletion of RTN neurons almost abolishes the reflex (Guyenet and Bayliss, 2015; Guyenet et al., 2016). Two proton-sensing molecules responsible for the CO_2 sensitivity of RTN neurons have been identified; a member of the two-pore domain potassium channel family, TASK-2, and a heterotrimeric guanine nucleotide-binding protein-coupled receptor, GPR-4 (Gestreau et al., 2010; Ludwig et al., 2003). Indeed, the central respiratory chemoreflex (ventilatory response to hyperoxic hypercapnia) was reduced by 90% in GPR-4 and TASK-2 double-knockout (KO) mice (Kumar et al., 2015). Conditional mouse mutants of $Phox2B^{27Ala}$, responsible for congenital central hypoventilation syndrome in humans, lack RTN neurons and they do not respond to hyperoxic hypercapnia at the neonatal stage but nevertheless survive (Ramanantsoa and Gallego, 2013). However, the central chemosensitivity partially recovers as these mutant mice mature (Ramanantsoa et al., 2011). Therefore, other chemosensing mechanisms may become functional through maturation.

Transient receptor potential (TRP) channels are polymodal cation channels that could function as sensors for pH, temperature, mechanical stressors and inflammatory metabolites (Nilius and Szallasi, 2014). TRP channels are divided into seven subfamilies: TRPC (canonical), TRPV (vanilloid), TRPM (melastatin), TRPML (mucolipin), TRPP (polycystin), TRPA (ankyrin) and TRPN (NomPC). TRPV1 is encoded as a capsaicin receptor that is not only activated by heat ($> 42\,^{\circ}C$) but also regulated by protons (Hellwig et al., 2004). TRPV4-expressing Chinese hamster ovary (CHO) cells are activated by extracellular pH (Suzuki et al., 2003), whereas TRPV4 activity in esophageal epithelial cells is suppressed by acidification (Shikano et al., 2011). Further, the sensitivity of TRPM8 to cold and menthol was reduced by an increase in proton concentration (Mahieu et al., 2010).

We previously reported that medullary glial cells showed a Ca^{2+} response to CO_2 through TRP channel-mediated mechanisms (Hirata and Oku, 2010). In particular, TRPM8 appeared to have the greatest CO_2 sensitivity. Thus, we hypothesized that TRP channels are involved in the central chemoreflex. To test this hypothesis, we examined

* Corresponding authors.
E-mail addresses: hiratayu@hyo-med.ac.jp (Y. Hirata), yoku@hyo-med.ac.jp (Y. Oku).

https://doi.org/10.1016/j.resp.2019.03.002
Received 4 February 2019; Received in revised form 22 February 2019; Accepted 4 March 2019
Available online 04 March 2019

ventilatory responses to hyperoxic hypercapnia in various TRP-KO mice by whole-body plethysmography. Furthermore, we evaluated Ca^{2+} responses to CO_2 in human embryonic kidney-293 (HEK-293) cells in which TRPM8 was overexpressed.

2. Materials and methods

2.1. Animals

TRPM8-, TRPV1- and TRPV4-deficient mice have been described in detail previously (Dhaka et al., 2007; Yoshiyama et al., 2015). These mice had been backcrossed on a C57BL/6Cr background, and 10 ~ 13-week-old male mice were used in this study. TRPM8-knockout (KO) mice were obtained from Dr. Patapoutian at the Scripps Research Institute, USA. TRPV1-KO mice were obtained from Dr. Julius at the University of California, USA. GFAP-EGFP transgenic (TG) mice expressing enhanced green fluorescent protein (EGFP) under a glial fibrillary acid protein (GFAP) promoter were obtained from Dr. Kirchhoff at the Max-Planck-Institute, Germany. All experiments were conducted according to the Regulations for Animal Experiments in Hyogo College of Medicine, the National Institute for Physiological Sciences, and the Fundamental Guidelines for Proper Conduct of Animal Experiments and Related Activities in Academic Research Institutions in Japan.

2.2. Whole-body plethysmography

The respiratory frequency (f_R, breaths min^{-1}), tidal volume (V_T, μL/g) and minute ventilation (MV, $f_R \times V_T$) in conscious, freely moving mice were measured using whole-body plethysmography as previously described in detail (Onodera et al., 1997; Trapp et al., 2011). We measured the rectal temperature substituted for the body temperature using an infrared thermometer (Laesent International Co., Center 352, China). In brief, mice in arousal cycle were placed in a recording chamber at dim place (160 mL) that was flushed continuously with a mixed gas containing 50% N_2 and 50% O_2 at a rate of 100 mL/min (temperature 24 ~ 26 °C) using a mass flow controller (MODEL8300, KOFLOC, Japan) and allowed 30 min to acclimate. Hyperoxic hypercapnia was induced by applying a gas mixture of 3 or 8% CO_2 with 50% O_2 (lowering N_2 accordingly). To measure the variation in the differential pressure in the chamber by ventilation, the chamber was fitted to a respiratory flow head (MLT1L) connected to a spirometer (ML140). The pressure signal was digitized and recorded using a PowerLab A/D converter and Chart v5.0 software (AD Instruments, USA). The measurements of the ventilatory variables were obtained during the 6 s periods (10 times) before exposure to the stimulus and during the 6 s periods (10 times) near the termination of each stimulus, when breathing had stabilized. The plethysmograph was calibrated by repeated exchanges of air (0.05, 0.1 mL and 0.2 mL) in the recording chamber. Hypercapnia-induced changes in f_R, V_T and MV were averaged and expressed as the mean ± SEM.

2.3. mRNA extraction and real-time PCR

GFAP-EGFP-TG mice (~10 weeks old) were administered anesthesia with 2 ~ 4% isoflurane by inhalation and their medullas were dissected out; half of the samples were shredded into RNA stabilization solution (RNA Save, Biological Industries, Israel) and stored overnight at 4 °C. The remaining half of the samples were incubated in Eagle's balanced salt solution containing papain (20 units/mL; Roche Diagnostics, Germany) for 30 min at 37 °C using modified methods described previously (Hirata and Oku, 2010). Single cells were subsequently isolated by trituration, washed three times with PBS (100 *g* for 5 min at 4 °C) and passed through a 35 μm Cell-Strainer (BD Falcon, USA). EGFP-positive cells were sorted on a FACSAria III (BD, Biosciences, USA) using the 488-nm excitation laser and 530/30 nm emission filter to detect the green fluorescence of EGFP. From EGFP-positive cells and the whole medulla, total RNA was isolated using a NucleoSpin RNA kit including DNase (Macherey-Nagel, Germany). cDNA was synthesized using the PrimeScript First Strand cDNA Synthesis Kit (Takara Bio, Japan). Quantitative real-time PCR was performed using 2.5 ng/μL cDNA, SYBR Premix Ex Taq II (Takara Bio, Japan) and 0.4 μM primers with the ABI 7900HT Fast Real-Time PCR System (Applied Biosystems, USA). Primers for the mouse samples were as follows: TRPM8 (f) 5′-acatcaagtaaggctggcg-3′ and (r) 5′-gggacctgaaaatgtctcctt-3′; TRPV1 (f) 5′-aactgtgagggcgtcaag-3′ and (r) 5′-gtgctatgcctatctcgagtg-3′; TRPV4 (f) 5′-cctggcaagagtgaaatctacc-3′ and (r) 5′-ttcttgttcagctccactacg-3′; S100B (f) 5′-ccctcattgatgtcttccacc-3′ and (r) 5′-tctccatcactttgtccacc-3′; and GAPDH (f) 5′-ctttgtcaagctcatttcctgg-3′ and (r) 5′-tcttgctcagtgtccttgc-3′. Gene expression was normalized by GAPDH as an internal control.

2.4. Generation of stable TRPM8-overexpressing HEK-293 cell lines

Full-length mouse TRPM8 cDNA was generated by the PCR Thermal Cycler Dice (Takara Bio, Japan) using the following primers: forward primer, 5′-gctagcgccaccatgtccttcgagggagccaggctcagcatg-3′ and reverse primer, 5′-ggccgcggccgctcttgatgttattagcaatctctttcagaa-3′. The 2A-peptides (forward oligo: 5′-ctagcgccaccatgagcggccgcaagattgtcgctcctgtcaaacaaactct-taactttgatttactcaaactggctggggatgtagaaagcaatccaggtccat-3′, reverse oligo: 5′-ctagatggacctggattgctttctacatccccagccagtttgagtaaatcaaagttaagagtttgtttga-caggagcgacaatcttgcggccgctcatggtggcg-3′) with or without full-length mouse TRPM8 cDNA were subcloned into pcDNA3.1-mCherry. mCherry and TRPM8 were separated by the 2A-peptide in bicistronic expression. The two constructed plasmids (pcDNA3.1-mCherry2A, pcDNA3.1-mCherry2A-TRPM8) were linearized with a restriction enzyme, PvuI, and then transfected into human embryonic kidney-293 (HEK-293) cells (ATCC, USA) using the electroporation system CUY21 Pro-Vitro (Nepagene, Japan). Stably transfected cell lines were selected in medium containing 500 μg/mL G418 for 10 days. To enrich mCherry2A-expressing cells with or without TRPM8, cells were sorted on a FACSAria III (BD, Biosciences, USA) using the 561-nm yellow-green excitation laser and 610/20 nm emission filter to detect the red fluorescence of mCherry and reseeded in growth medium.

2.5. Measurements of intracellular Ca^{2+}

The intracellular Ca^{2+} level in mCherry2A-expressing or mCherry2A-TRPM8-expressing HEK-293 cells was recorded using the Ca^{2+} indicator Fluo-8H. Cells on glass-bottom dishes (Matsunami, Japan) were loaded with the acetoxymethyl (AM) ester of Fluo-8H (5 μM) in artificial cerebrospinal fluid (aCSF) carbogen saturated with a CO_2 incubator (5%) for 30 min at 37 °C, as previously described (Hirata and Oku, 2010). The aCSF solution contained (in mM) 124 NaCl, 5 KCl, 2.4 $CaCl_2$, 1.3 $MgCl_2$, 1.2 KH_2PO4, 26 $NaHCO_3$ and 30 glucose and was equilibrated with either 5% CO_2–95% O_2 (control solution) or 12% CO_2–88% O_2 (hypercapnic solution) at 35 °C. After a wash step, the cells were continuously superfused with aCSF bubbled with 5% CO_2–95% O_2 at a rate of ~0.8 mL/min for 5 ~ 10 min at 35 °C before experiments. The fluorescence signal of Fluo-8H was imaged by a confocal microscope Zeiss LSM510 (Axiovert 200M, Carl Zeiss, Germany). The acquired images (512 × 512 pixels) were transferred to MATLAB software, the individual cells in a field were identified automatically as previously described (Oku et al., 2016), and the peak Ca^{2+} response in each cell was detected by the algorithm. The fluorescence intensity ($\Delta F/F_0$) was expressed as the ratio of the change in fluorescence (ΔF) signal to the average value of the fluorescence (F_0) signal at baseline, 5 s after the initiation of measurement.

2.6. Statistical analysis

All data are presented as the mean ± SEM. The difference between the groups was calculated by student's *t*-test or one-way ANOVA. Origin Pro9.0 software was used for statistical analysis, and a P-value lower

than 0.05 or 0.01 was considered significant.

3. Results

3.1. Ventilatory responses to hypercapnia in TRPM8-KO mice

Under resting conditions (normocapnia), respiratory frequency (f_R) was not significantly different between adult wild-type mice (WT: 164.5 ± 2.60 min^{-1}, n = 61) and TRPM8-KO mice (M8-/-: 157.1 ± 3.21 min^{-1}, n = 40, p = 0.076), but there was a significant difference in tidal volume (V_T; WT: 7.27 ± 0.21 μL/g, n = 61, M8-/-: 6.32 ± 0.21 μL/g, n = 40, p < 0.01) and minute ventilation (MV; WT: 1.20 ± 0.04 mL/g/min, n = 61, M8-/-: 0.99 ± 0.04 mL/g/min, n = 40, p < 0.01). There was no significant difference between 13-week-old WT mice and TRPM8-KO mice in body weight (WT: 26.78 ± 0.29 g, n = 43, M8-/-: 27.34 ± 0.35 g, n = 42, p = 0.222) and body temperature (WT: 32.07 ± 0.23 °C, n = 43, M8-/-: 32.29 ± 0.29 °C, n = 42, p = 0.574). When exposed to hypercapnic conditions, both WT mice and TRPM8-KO mice showed an increased f_R and V_T and, therefore, an increased MV ($f_R \times V_T$). This hypercapnia-induced increase in ventilation was markedly reduced in TRPM8-KO mice (Fig. 1B). Thus, in a mixed gas of 3% or 8% CO_2 with 50% O_2, MV in WT mice increased to 1.73 ± 0.10 mL/g/min (n = 29) and 3.40 ± 0.10 mL/g/min (n = 61), respectively, whereas in the TRPM8-KO mice under the same conditions, MV was elevated to 1.23 ± 0.05 mL/g/min (n = 29, p < 0.01) and 2.26 ± 0.13 mL/g/min (n = 40, p < 0.01), respectively (Fig. 1B). In addition, we compared the ventilatory response to hypercapnia in TRPM8-KO mice with that in other TRP-deficient mice (V1-/- or V4-/-). There was a significant difference in hypercapnic responses between TRPM8-KO mice and WT mice. The increased rate of MV induced by 8% CO_2 in TRPM8-KO mice (n = 40) remarkably decreased to 66.4% of that in WT mice (n = 61, p < 0.01).

However, the rate of MV in TRPV1-KO mice slightly increased to 116.4% (n = 13, p = 0.085) of that in WT mice, and that of TRPV4-KO mice slightly decreased to 95.4% (n = 19, p = 0.862) of that in WT mice (Fig. 1C). The body weight of 13-week-old TRPV1-KO mice (27.96 ± 0.77 g, n = 13, p = 0.89) was not significantly different from that of WT mice, but that of 13-week-old TRPV4-KO mice (29.19 ± 0.55 g, n = 19, p < 0.01) increased significantly. Unexpectedly, even in normocapnia, the MV and V_T of TRPM8-KO mice were significantly reduced compared with those of WT mice but not those of other TRP-deficient mice (Fig. 1B and C).

3.2. Comparison of TRP subtype gene expression in glial cells of the medulla

To detect the expression of TRP channels in glial cells of the medulla, we sorted EGFP-positive cells from the medulla of GFAP-EGFP-TG mice, in which EGFP expression in glial cells is driven by the GFAP promoter. As shown in Fig. 2, S100B as a glial cell marker was increased by 62.8-fold in the sorted EGFP-positive cells compared with the whole medulla when GAPDH was used as an internal standard. Similarly, TRPM8 and TRPV4 levels were significantly increased in the EGFP-positive cells by 1.5- and 13.3-fold, respectively, but the TRPV1 level was not increased.

3.3. Hypercapnic acidosis-induced Ca^{2+} response mediated by TRPM8

To verify whether hypercapnic acidosis induces Ca^{2+} responses through TRPM8, we generated a stable HEK-293 cell line over-expressing TRPM8. This mCherry2A-TRPM8-expressing cell line bicistronically expressed mCherry and TRPM8 proteins by the 2A self-cleaving peptide. The control of this cell is mCherry2A-expressing cell line and expresses mCherry without TRPM8. In the mCherry2A-expressing cells, hypercapnic acidosis-induced Ca^{2+} responses were observed in 107 cells (5%), and menthol-induced responses were observed in 211 cells (10%). However, in mCherry2A-TRPM8-expressing cells, hypercapnic acidosis-induced Ca^{2+} responses were observed in 839 cells (38%), and menthol-induced Ca^{2+} responses were observed in 1219 cells (54%). Following exposure to hypercapnic acidosis, the peak Ca^{2+} response in mCherry2A-TRPM8-expressing cells was significantly higher than that in control cells (31.92 ± 0.83 vs 6.00 ± 1.36 $\Delta F/F_0$ %, p < 0.01). The peak menthol-induced Ca^{2+} responses were 39.06 ± 0.61 and 19.54 ± 0.97 ($\Delta F/F_0$ %) in mCherry2A-TRPM8-expressing cells and control cells, respectively, and the difference was statistically significant (p < 0.01) (Fig. 3A and B).

4. Discussion

4.1. Expression of TRP subtypes in the medulla

We previously reported that TRP channels mediate hypercapnic Ca^{2+} responses in glia-rich medullary cultures independent of extracellular pH (Hirata and Oku, 2010). Here, we examined the expression of TRP subtypes in glial cells in the medulla by using GFAP-EGFP-TG mice and detected the expression of TRPM8, TRPV1 and TRPV4 in EGFP-positive glial cells, although their expression levels were different. In the literature, among TRP subtypes such as TRPM, TRPV, and TRPC families, TRPM8 showed the highest upregulation in glioblastoma compared with normal brain tissue (Alptekin et al., 2015), although the physiological role of TRPM8 in the brain has been scarcely reported. Recently, it has been reported that cold stress as well as cerebral ischemia induces the expression of TRPM8 in the mouse brain (Wang et al., 2017). In addition, another literature has reported that glia-rich medullary cultures express TRPM8 and include hypercapnic Ca^{2+}-responsive cells (Hirata and Oku, 2010). These findings support the hypothesis that TRPM8 mediates hypercapnic Ca^{2+} responses in medullary glial cells.

TRPV4 expression has been described in various cell types of the nervous system, including dorsal root ganglion neurons (Gao and Wang, 2010), hippocampal neurons (Shibasaki et al., 2015), medulla oblongata (Onishi et al., 2018) and glial cells (Shibasaki et al., 2014). In this study, the expression ratio of TRPV4 to S100B was approximately 21%, which was similar to that reported by Shibasaki et al. (2014). A recent report indicated that TRPV1 is expressed in various brain regions, such as neuronal, glial and microglial cells, but the expression level in glial cells is very low (Marrone et al., 2017). Similarly, in our experiments, the expression level of glial TRPV1 was the lowest. These findings suggest that the contribution of TRPV1 might be small.

4.2. Involvement of TRPM8 in the ventilatory response to CO_2

Although TRPM8 was not strongly expressed in glial cells of the medulla, in the ventilatory response to hypercapnia, the MV in TRPM8-KO mice with 8% CO_2 was significantly reduced to approximately 66% of that in WT mice. In both TASK-2-KO mice and GPR4-KO mice, tidal volume (V_T) response to 8% CO_2 decreased to approximately 65% of WT (Kumar et al., 2015; Guyenet et al., 2016). Reduction of the hypercapnic response in these KO mice was comparable to that in TRPM8-KO mice (~66%).

GPR-4 and TASK-2 double-KO mice showed an almost completely abolished hypercapnic response (90% reduction) (Kumar et al., 2015; Guyenet et al., 2016). Approximately 73% of Phox2B-expressing cells expressed both GPR-4 and TASK-2 (Kumar et al., 2015). Thus, the elimination of Phox2B-expressing RTN neurons also causes a nearly complete loss of CO_2 sensitivity (Ramanantsoa et al., 2011). However, surprisingly, the hypercapnic response was restored in adult Phox2B^{27Ala} mutant mice to 60% of the level in WT mice. In the steady-state respiration of Phox2B^{27Ala} mutant mice, the V_T of the Phox2B^{27Ala} mutant neonates decreased to 40% of that in WT neonates, but the V_T of Phox2B^{27Ala} mutant adult mice recovered to a normal level (Ramanantsoa et al., 2011). The steady-state respiration of GPR-4 and

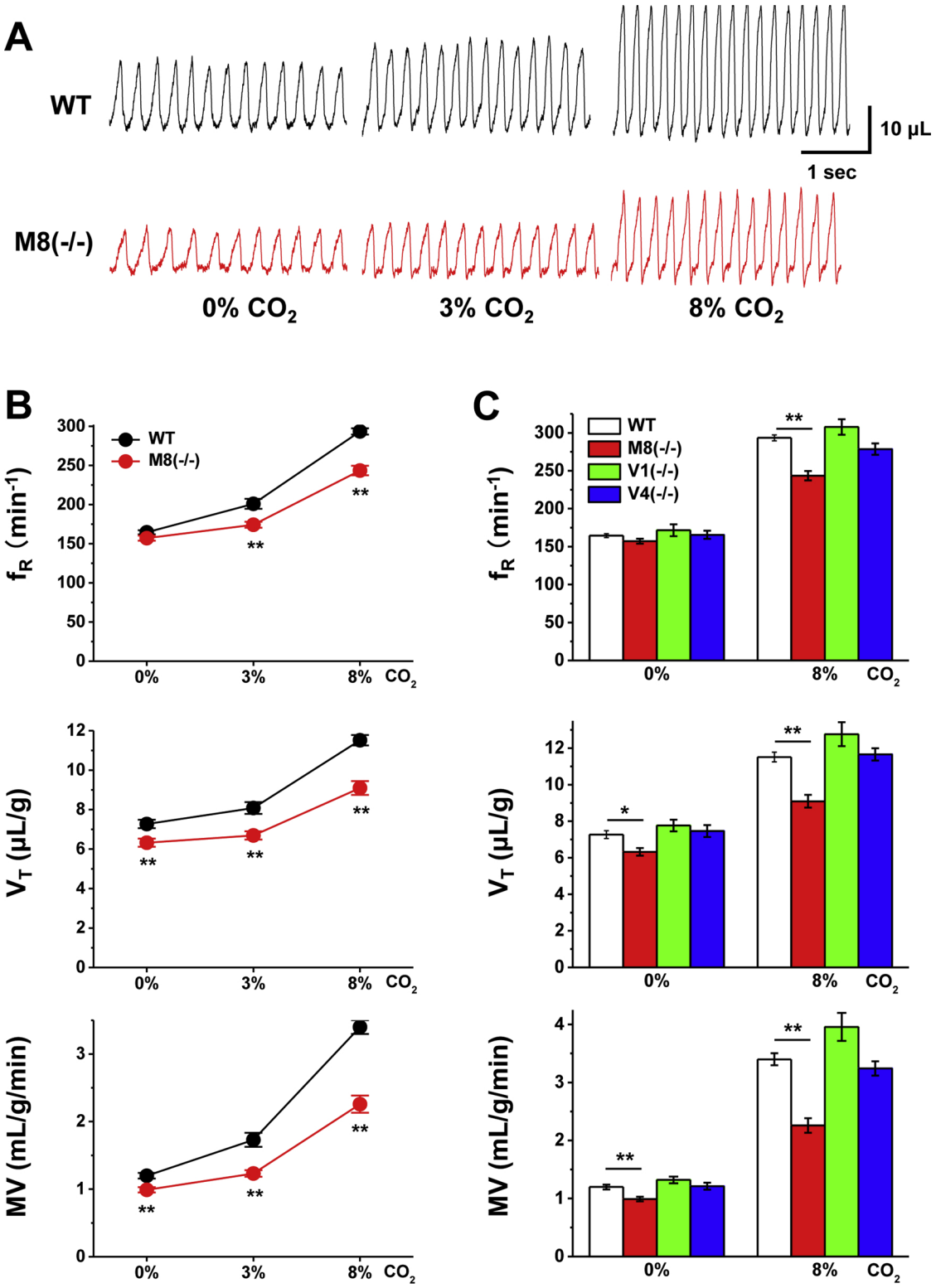

Fig. 1. Ventilatory responses to hypercapnia in TRPM8-, TRPV1- and TRPV4-deficient mice. (A) Representative plethysmography traces of wild-type (WT) and TRPM8-deficient (M8(-/-)) mice in both normocapnia (0% CO_2) and hypercapnia (3%, 8% CO_2). (B) Mean values of the respiratory frequency (f_R, min^{-1}), tidal volume (V_T, μL/g) and minute ventilation (MV, mL/g/min) of the animals shown in A. At 3% or 8% CO_2, the f_R, V_T and MV of M8(-/-) mice were significantly attenuated compared with those of WT mice. Data are presented as the mean ± SEM. ** $P < 0.01$ (student's *t*-test). (C) Comparison of ventilatory responses to normocapnia (0% CO_2) and hypercapnia (8% CO_2) between TRPM8-, TRPV1- and TRPV4-deficient mice and WT mice. Data are presented as the mean ± SEM. At 0% or 8% CO_2, the population variance in f_R, V_T, and MV among WT, M8(-/-), V1(-/-) and V4(-/-) mice was not significantly different ($P > 0.01$). At 0% CO_2, there was a significant difference in V_T and MV among WT, M8(-/-), V1(-/-) and V4(-/-) mice [$F(3, 5.11) < 0.01$, $p < 0.05$], [$F(3, 6.67) < 0.01$, $p < 0.01$], respectively. At 8% CO_2, there was a significant difference in f_R, V_T, and MV among WT, M8(-/-), V1(-/-) and V4(-/-) mice [$F(3, 21.23) < 0.01$, $p < 0.01$], [$F(3, 16.61) < 0.01$, $p < 0.01$], [$F(3, 25.05) < 0.01$, $p < 0.01$], respectively. *$P < 0.05$ and ** $P < 0.01$ (one-way ANOVA and Tukey's multiple comparison test).

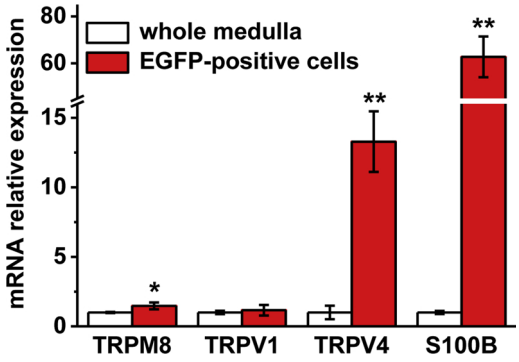

Fig. 2. TRP subtype gene expression in glia of the medulla. Quantification of TRPM8, TRPV1, TRPV4 and S100B mRNAs normalized by GAPDH in the whole medulla (white bars) and in EGFP-positive cells from the medulla (red bars). Data are presented as the mean ± SEM. (n = 5~12). Asterisks indicate a significant difference in the relative increase in mRNA expression in EGFP-positive cells compared to the whole medulla using student's *t*-test. * P < 0.05 and ** P < 0.01.

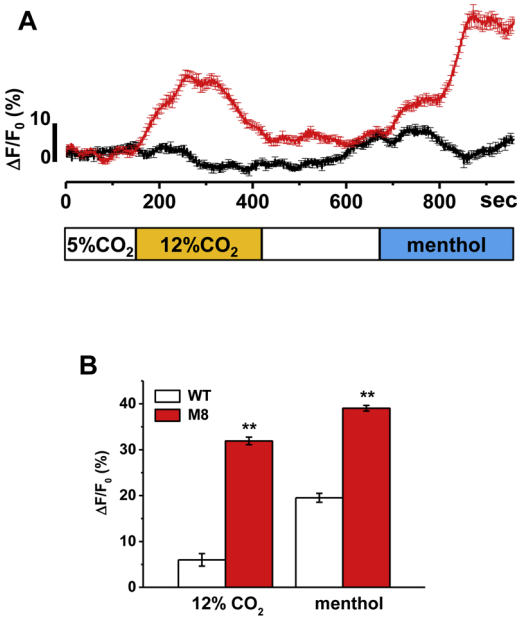

Fig. 3. Ca^{2+} responses to hypercapnic acidosis and menthol in TRPM8-overexpressing HEK-293 cells. (A) Averaged traces of Ca^{2+} responses (with SEM at every third point) using Fluo-8H AM upon hypercapnic acidosis followed by menthol (0.1 mM) in mCherry2A-expressing HEK-293 cells as a control (black trace, n = 374) and mCherry2A-TRPM8-expressing HEK-293 cells (red trace, n = 303). The control condition was HCO_3^--buffered solution (5% CO_2, 26 mM HCO_3^-, pHo 7.4) for hypercapnic acidosis (12% CO_2, 26 mM HCO_3^-, pHo 7.1). (B) Summary of mean peak Ca^{2+} responses ($\Delta F/F_0$ %) induced by hypercapnic acidosis (12% CO_2) or menthol (0.1 mM) in control cells (WT, 6 independent experiments; n = 2226) and TRPM8-overexpressing HEK-293 cells (M8, 6 independent experiments; n = 2219). Data are presented as the mean ± SEM. ** P < 0.01 (student's *t*-test).

TASK-2 double-KO mice was also normal in adult mice (Kumar et al., 2015; Guyenet et al., 2016; Santin, 2018). These results suggest that alternative mechanisms might compensate for the loss of CO_2 sensitivity during development. Interestingly, we found that in adult TRPM8-KO mice, the V_T was slightly but significantly reduced even in steady-state respiration. Furthermore, the proportion of TRPM8-expressing cells in the trigeminal ganglion increases with age (Alcalde et al., 2018). Therefore, although the CO_2 chemosensitivity in steady-state respiration seems to be predominantly mediated by GPR-4 and TASK-2 in neonates, a part of the CO_2 chemosensitivity might be attributed to TRPM8 in adults.

Because TRPM8 is also expressed on airway afferent nerves, which initiate the response to cold air and causes autonomic responses such as bronchoconstriction, cough and mucus secretion (Plevkova, 2012), the possible involvement of the peripheral response by the airway afferent nerve cannot be excluded in the reduction of the CO_2 ventilatory response in TRPM8-KO mouse. Menthol centrally inhibits respiratory rhythm generation in brainstem-spinal cord preparations (Tani et al., 2010). Menthol is a known agonist of TRPM8, while it activates the GABA receptor directly in the hippocampus (Zhang et al., 2008). Indeed, the inhibitory effect of menthol on respiratory rhythm generation in brainstem-spinal cord preparations is mediated through the direct activation of GABAergic neurons (Tani et al., 2010).

4.3. Involvement of TRPV1 and TRPV4 in the ventilatory response to CO_2

Tani et al. (2017) indicated that capsaicin, a specific agonist of TRPV1, increased the fluctuation of the membrane potential in CO_2-sensitive pre-inspiratory neurons. These researchers suggested that there is a minor contribution of the TRPV1 channels to central chemoreception. Similarly, our results indicated that both the ventilatory responses (f_R and V_T) to 0% CO_2 and 8% CO_2 in TRPV1-KO mice slightly increased compared to WT, but the difference was not significant. TRPV4 can function as Ca^{2+}-permeable cation channels that are gated by various stimuli, such as cell swelling, low pH, mechanical stress and temperature (White et al., 2016). Several researchers report that not only CO_2 but also H^+ trigger the central chemoreflex (Guyenet and Bayliss, 2015), leading to suggestion that pH sensitivity of TRPV4 act as a sensor of central chemoreflex. TRPV4-expressing astrocytes release ATP and glutamate to regulate neurons (Shibasaki et al., 2014). In the medulla, glial TRPV4 could alter the neuronal activity of nucleus tractus solitaries that regulates arterial pressure levels (Onishi et al., 2018). However, although TRPV4 was highly expressed in medullary glial cells, we could not find any difference in ventilatory response to CO_2 in TRPV4-KO mice compared to WT.

4.4. Ca^{2+} response through TRPM8

Our previous studies have shown that hypercapnic Ca^{2+} responses are mediated through TRP channels including TRPM8 in glial cells of the medulla (Hirata and Oku, 2010). This observation is consistent with that of the present study, in which TRPM8 is involved in the ventilatory response to CO_2 *in vivo*. We examined whether TRPM8 was sensitive to CO_2 *in vitro* and found transient Ca^{2+} responses upon hypercapnic stimulation. Furthermore, among the TRPM8-expressing cells, a Ca^{2+} response induced by menthol was observed in 54%, but a Ca^{2+} response induced by CO_2 was observed in 38%. This finding suggests that, as shown in our previous report, not all TRPM8 channels expressed in HEK-293 cells have CO_2 sensitivity. There are reports that would be helpful in interpreting this heterogeneous response of TRPM8. Since N-glycosylation of TRPM8 modulates Ca^{2+} response to menthol as well as cold stimuli (Pertusa et al., 2012), the difference in the state of N-glycosylation in each glial cell might change CO_2 sensitivity. Further, glioma cell migration and mitosis are regulated by reciprocal and interdependent activities of Ca^{2+}-activated intermediate conductance K^+ channels, big conductance K^+ channels, and TRPM8. There is also a possibility that TRPM8 is regulated differently depending on the conjugated molecule (Klumpp et al., 2017). Another report shows that activation of TRPM8 by menthol and cold stimulation is inhibited not only by heat stimulation but also by capsaicin (TRPV1 agonist) (Takaishi et al., 2016). These findings suggest that molecule coupling or the interaction with other TRP subtypes and/or ion channels may attenuate the CO_2 chemosensitivity of TRPM8.

In conclusion, our study found for the first time that TRPM8-KO mice have a decreased ventilatory response to CO_2. Although the ventilatory response to CO_2 has almost completely disappeared in GPR-4

and TASK-2 double-KO mice, steady-state respiration of these KO mice is normal, suggesting that inhaled CO_2 and metabolic CO_2 induce a ventilatory response by different CO_2 chemosensitivity (Santin, 2018). On the other hand, adult TRPM8-KO mice showed a significant attenuation in steady-state ventilation but no metabolic difference such as body weight and body temperature, suggesting that the attenuation of CO_2 sensitivity was not due to a decrease in metabolic CO_2. In addition, there are reports that astrocytic connexin 26, ATP and PGE2 are involved in ventilatory response to CO_2 (Gourine et al., 2010; Forsberg et al., 2016), and it is unlikely that one type of molecule is responsible for CO_2 chemosensitivity. Taken together, our results suggest that CO_2 chemosensitivity involves TRPM8 regulated by conjugated molecules dependent on hypercapnia and steady-state respiration.

Conflicts of interest

The authors declare that there are no conflicts of interest.

Acknowledgments

This work was supported by Grant-in-Aid for Scientific Research Grants (KAKENHI)23590292 and 21790231 (Y.H.), Planned collaborative project of National Institute for Physiological Sciences (Y.H.), and Grant-in-Aid for Researchers, Hyogo College of Medicine, 2016 (Y.H.). We thank Shigefumi Yokota for the useful discussions, and Tomio Nakajima and Michie Tabata for the technical support.

References

Alcalde, I., Inigo-Portugues, A., Gonzalez-Gonzalez, O., Almaraz, L., Artime, E., Morenilla-Palao, C., Gallar, J., Viana, F., Merayo-Lloves, J., Belmonte, C., 2018. Morphological and functional changes in TRPM8-expressing corneal cold thermoreceptor neurons during aging and their impact on tearing in mice. J. Comp. Neurol. 526, 1859–1874. https://doi.org/10.1002/cne.24454.

Alptekin, M., Eroglu, S., Tutar, E., Sencan, S., Geyik, M.A., Ulasli, M., Demiryurek, A.T., Camci, C., 2015. Gene expressions of TRP channels in glioblastoma multiforme and relation with survival. Tumor Biol. 36, 9209–9213. https://doi.org/10.1007/s13277-015-3577-x.

Dhaka, A., Murray, A.N., Mathur, J., Earley, T.J., Petrus, M.J., Patapoutian, A., 2007. TRPM8 is required for cold sensation in mice. Neuron 54, 371–378. https://doi.org/10.1016/j.neuron.2007.02.024.

Forsberg, D., Horn, Z., Tserga, E., Smedler, E., Silberberg, G., Shvarev, Y., Kaila, K., Uhlen, P., Herlenius, E., 2016. CO2-evoked release of PGE2 modulates sighs and inspiration as demonstrated in brainstem organotypic culture. Elife 5. https://doi.org/10.7554/elife.14170.

Gao, F., Wang, D.H., 2010. Hypotension induced by activation of the transient receptor potential vanilloid 4 channels: role of Ca2+-activated K+ channels and sensory nerves. J. Hypertens. 28, 102–110. https://doi.org/10.1097/HJH.0b013e328332b865.

Gestreau, C., Heitzmann, D., Thomas, J., Dubreuil, V., Bandulik, S., Reichold, M., Bendahhou, S., Pierson, P., Sterner, C., Peyronnet-Roux, J., Benfriha, C., Tegtmeier, I., Ehnes, H., Georgieff, M., Lesage, F., Brunet, J.-F., Goridis, C., Warth, R., Barhanin, J., 2010. Task2 potassium channels set central respiratory CO2 and O2 sensitivity. Proc. Natl. Acad. Sci. U. S. A. 107, 2325–2330. https://doi.org/10.1073/pnas.0910059107.

Gourine, A.V., Kasymov, V., Marina, N., Tang, F., Figueiredo, M.F., Lane, S., Teschemacher, A.G., Spyer, K.M., Deisseroth, K., Kasparov, S., 2010. Astrocytes control breathing through pH-dependent release of ATP. Science 329, 571–575. https://doi.org/10.1126/science.1190721.

Guyenet, P.G., Bayliss, D.A., 2015. Neural control of breathing and CO2 homeostasis. Neuron 87, 946–961. https://doi.org/10.1016/j.neuron.2015.08.001.

Guyenet, P.G., Bayliss, D.A., Stornetta, R.L., Ludwig, M.G., Kumar, N.N., Shi, Y.T., Burke, P.G.R., Kanbar, R., Basting, T.M., Holloway, B.B., Wenker, I.C., 2016. Proton detection and breathing regulation by the retrotrapezoid nucleus. J. Physiol. 594, 1529–1551. https://doi.org/10.1113/jp271480.

Hellwig, N., Plant, T.D., Janson, W., Schafer, M., Schultz, G.N., Schaefer, M., 2004. TRPV1 acts as proton channel to induce acidification in nociceptive neurons. J. Biol. Chem. 279, 34553–34561. https://doi.org/10.1074/jbc.M402966200.

Hirata, Y., Oku, Y., 2010. TRP channels are involved in mediating hypercapnic Ca2+ responses in rat glia-rich medullary cultures independent of extracellular pH. Cell Calcium 48, 124–132. https://doi.org/10.1016/j.ceca.2010.07.006.

Klumpp, D., Frank, S.C., Klumpp, L., Sezgin, E.C., Eckert, M., Edalat, L., Bastmeyer, M., Zips, D., Ruth, P., Huber, S.M., 2017. TRPM8 is required for survival and radioresistance of glioblastoma cells. Oncotarget 8, 95896–95913. https://doi.org/10.18632/oncotarget.21436.

Kumar, N.N., Velic, A., Soliz, J., Shi, Y.T., Li, K.Y., Wang, S., Weaver, J.L., Sen, J., Abbott, S.B.G., Lazarenko, R.M., Ludwig, M.G., Perez-Reyes, E., Mohebbi, N., Bettoni, C., Gassmann, M., Suply, T., Seuwen, K., Guyenet, P.G., Wagner, C.A., Bayliss, D.A., 2015. Regulation of breathing by CO2 requires the proton-activated receptor GPR4 in retrotrapezoid nucleus neurons. Science 348, 1255–1260. https://doi.org/10.1126/science.aaa0922.

Ludwig, M.-G., Vanek, M., Guerini, D., Gasser, J.A., Jones, C.E., Junker, U., Hofstetter, H., Wolf, R.M., Seuwen, K., 2003. Proton-sensing G-protein-coupled receptors. Nature 425, 93–98. https://doi.org/10.1038/nature01905.

Mahieu, F., Janssens, A., Gees, M., Talavera, K., Nilius, B., Voets, T., 2010. Modulation of the cold-activated cation channel TRPM8 by surface charge screening. J. Physiol. 588, 315–324. https://doi.org/10.1113/jphysiol.2009.183582.

Marrone, M.C., Morabito, A., Giustizieri, M., Chiurchiu, V., Leuti, A., Mattioli, M., Marinelli, S., Riganti, L., Lombardi, M., Murana, E., Totaro, A., Piomelli, D., Ragozzino, D., Oddi, S., Maccarrone, M., Verderio, C., 2017. TRPV1 channels are critical brain inflammation detectors and neuropathic pain biomarkers in mice. Nat. Commun. 8. https://doi.org/10.1038/ncomms15292.

Nattie, E., Li, A.H., 2012. Central chemoreceptors: locations and functions. Compr. Physiol. 2, 221–254. https://doi.org/10.1002/cphy.c100083.

Nilius, B., Szallasi, A., 2014. Transient receptor potential channels as drug targets: from the science of basic research to the art of medicine. Pharmacol. Rev. 66, 676–814. https://doi.org/10.1124/pr.113.008268.

Oku, Y., Fresemann, J., Miwakeichi, F., Hulsmann, S., 2016. Respiratory calcium fluctuations in low-frequency oscillating astrocytes in the pre-Botzinger complex. Respir. Physiol. Neurobiol. 226, 11–17. https://doi.org/10.1016/j.resp.2015.02.002.

Onishi, M., Yamanaka, K., Miyamoto, Y., Waki, H., Gouraud, S., 2018. Trpv4 involvement in the sex differences in blood pressure regulation in spontaneously hypertensive rats. Physiol. Genomics 50, 272–286. https://doi.org/10.1152/physiolgenomics.00096.2017.

Onodera, M., Kuwaki, T., Kumada, M., Masuda, Y., 1997. Determination of ventilatory volume in mice by whole body plethysmography. Jpn. J. Physiol. 47, 317–326. https://doi.org/10.2170/jjphysiol.47.317.

Pertusa, M., Madrid, R., Morenilla-Palao, C., Belmonte, C., Viana, F., 2012. N-glycosylation of TRPM8 ion channels modulates temperature sensitivity of cold thermoreceptor neurons. J. Biol. Chem. 287, 18218–18229. https://doi.org/10.1074/jbc.M111.312645.

Plevkova, J., 2012. Thermo sensitive TRPM8 channel and its role in cold induced airway symptoms. Open J. Mol. Integr. Physiol. https://doi.org/10.4236/ojmip.2012.21004.

Ramanantsoa, N., Gallego, J., 2013. Congenital central hypoventilation syndrome. Respir. Physiol. Neurobiol. 189, 272–279. https://doi.org/10.1016/j.resp.2013.05.018.

Ramanantsoa, N., Hirsch, M.R., Thoby-Brisson, M., Dubreuil, V., Bouvier, J., Ruffault, P.L., Matrot, B., Fortin, G., Brunet, J.F., Gallego, J., Goridis, C., 2011. Breathing without CO2 chemosensitivity in conditional Phox2b mutants. J. Neurosci. 31, 12880–12888. https://doi.org/10.1523/jneurosci.1721-11.2011.

Santin, J.M., 2018. How important is the CO2 chemoreflex for the control of breathing? Environmental and evolutionary considerations. Comp. Biochem. Physiol. A Mol. Integr. Physiol. 215, 6–19. https://doi.org/10.1016/j.cbpa.2017.09.015.

Shibasaki, K., Ikenaka, K., Tamalu, F., Tominaga, M., Ishizaki, Y., 2014. A novel subtype of astrocytes expressing TRPV4 (transient receptor potential vanilloid 4) regulates neuronal excitability via release of gliotransmitters. J. Biol. Chem. 289, 14470–14480. https://doi.org/10.1074/jbc.M114.557132.

Shibasaki, K., Tominaga, M., Ishizaki, Y., 2015. Hippocampal neuronal maturation triggers post-synaptic clustering of brain temperature-sensor TRPV4. Biochem. Biophys. Res. Commun. 458, 168–173. https://doi.org/10.1016/j.bbrc.2015.01.087.

Shikano, M., Ueda, T., Kamiya, T., Ishida, Y., Yamada, T., Mizushima, T., Shimura, T., Mizoshita, T., Tanida, S., Kataoka, H., Shimada, S., Ugawa, S., Joh, T., 2011. Acid inhibits TRPV4-mediated Ca2+ influx in mouse esophageal epithelial cells. Neurogastroenterol. Motil. 23, 1020–e497. https://doi.org/10.1111/j.1365-2982.2011.01767.x.

Suzuki, M., Mizuno, A., Kodaira, K., Imai, M., 2003. Impaired pressure sensation in mice lacking TRPV4. J. Biol. Chem. 278, 22664–22668. https://doi.org/10.1074/jbc.M302561200.

Takaishi, M., Uchida, K., Suzuki, Y., Matsui, H., Shimada, T., Fujita, F., Tominaga, M., 2016. Reciprocal effects of capsaicin and menthol on thermosensation through regulated activities of TRPV1 and TRPM8. J. Physiol. Sci. 66, 143–155. https://doi.org/10.1007/s12576-015-0427-y.

Tani, M., Onimaru, H., Ikeda, K., Kawakami, K., Homma, I., 2010. Menthol inhibits the respiratory rhythm in brainstem preparations of the newborn rats. Neuroreport 21, 1095–1099. https://doi.org/10.1097/WNR.0b013e3283405bad.

Tani, M., Kotani, S., Hayakawa, C., Lin, S.T., Irie, S., Ikeda, K., Kawakami, K., Onimaru, H., 2017. Effects of a TRPV1 agonist capsaicin on respiratory rhythm generation in brainstem-spinal cord preparation from newborn rats. Pflugers Arch. J. Physiol. 469, 327–338. https://doi.org/10.1007/s00424-016-1912-8.

Trapp, S., Tucker, S.J., Gourine, A.V., 2011. Respiratory responses to hypercapnia and hypoxia in mice with genetic ablation of Kir5.1 (Kcnj16). Exp. Physiol. 96, 451–459. https://doi.org/10.1113/expphysiol.2010.055848.

Wang, X.P., Yu, X., Yan, X.J., Lei, F., Chai, Y.S., Jiang, J.F., Yuan, Z.Y., Xing, D.M., Du, L.J., 2017. TRPM8 in the negative regulation of TNF alpha expression during cold stress. Sci. Rep. 7. https://doi.org/10.1038/srep45155.

White, J.P.M., Cibelli, M., Urban, L., Nilius, B., McGeown, J.G., Nagy, I., 2016. TRPV4: molecular conductor of a diverse orchestra. Physiol. Rev. 96, 911–973. https://doi.org/10.1152/physrev.00016.2015.

Yoshiyama, M., Mochizuki, T., Nakagomi, H., Miyamoto, T., Kira, S., Mizumachi, R., Sokabe, T., Takayama, Y., Tominaga, M., Takeda, M., 2015. Functional roles of TRPV1 and TRPV4 in control of lower urinary tract activity: dual analysis of behavior and reflex during the micturition cycle. Am. J. Physiol. Physiol. 308, F1128–F1134. https://doi.org/10.1152/ajprenal.00016.2015.

Zhang, X.B., Jiang, P., Gong, N., Hu, X.L., Fei, D., Xiong, Z.Q., Xu, L., Xu, T.L., 2008. A-type GABA receptor as a central target of TRPM8 agonist menthol. PLoS One 3. https://doi.org/10.1371/journal.pone.0003386.